Why solidification has an S-shaped history

Adrian Bejan, Sylvie Lorente, B. S. Yilbas, A. Z. Sahin

SCIENTIFIC REPORTS

OPEN

SUBJECT AREAS:
MECHANICAL ENGINEERING
APPLIED PHYSICS
SCALING LAWS
THERMODYNAMICS

Received
27 December 2012

Accepted
9 April 2013

Published
26 April 2013

Why solidification has an S-shaped history

A. Bejan[1], S. Lorente[2], B. S. Yilbas[3] & A. Z. Sahin[3]

[1]Duke University, Department of Mechanical Engineering and Materials Science, Durham, North Carolina 27708-0300, USA, [2]University of Toulouse, INSA, LMDC (Laboratoire Matériaux et Durabilité des Constructions), 135 Avenue de Rangueil, 31077 Toulouse, France, [3]King Fahd University of Petroleum and Minerals, Mechanical Engineering Department, Dhahran, 31261, Saudi Arabia.

Correspondence and requests for materials should be addressed to A.B. (abejan@duke.edu)

Here we show theoretically that the history of solid growth during "rapid" solidification must be S-shaped, in accord with the constructal law of design in nature. In the beginning the rate of solidification increases and after reaching a maximum it decreases monotonically as the volume of solid tends toward a plateau. The S-history is a consequence of four configurations for the flow of heat from the solidification front to the subcooled surroundings, in this chronological order: solid spheres centered at nucleation sites, needles that invade longitudinally, radial growth by conduction, and finally radial lateral conduction to interstices that are warming up. The solid volume (B_s) vs time (t) is an S-curve because it is a power law of type $B_s \sim t^n$ where the exponent n first increases and then decreases in time (n = 3/2, 2, 1, …). The initial portion of the S curve is not an exponential.

An extremely common phenomenon in nature is the S-shaped history of areas and volumes swept by spreading flows and collecting flows. Examples of S-curve spreading histories are the growth of populations[1], the spreading of technologies[2], and the spreading of news and information[3], Fig. 1. The histories of collecting flows also exhibit S curves: examples are mining and the extraction of minerals, such as the Hubbert peak of oil extraction[4].

Rapid solidification is another common phenomenon, where the S-curve history is about the growth of solid in a subcooled liquid or gas. This phenomenon is classical textbook material in materials science[5–7], and has generated a voluminous body of research dedicated to explaining the S-shaped history. The classical explanation is based on the Johnson-Mehl-Avrami (JMA) model of solidification[8–13], which consists of postulating solidification as a swarm of uniformly distributed spheres of solid that grow from initial nucleation sites, such that initially the solid volume increases exponentially. Although this model leads to a formula with two empirical constants that can be used to correlate experimental measurements, the S-curve remains a theoretical puzzle, while the theoretical basis of the sphere model is being questioned[8]: the physical meaning of the two empirical constants is not known.

In this paper we go back to the state of knowledge that existed before the JMA model, and show how to predict the S-curve of solidification purely theoretically. The starting idea is to see solidification as a "spreading flow" like the flows exhibited in Fig. 1, and to recognize that this spreading flow has the same natural tendency as all the inanimate and animate flow systems that morph freely into configurations that provide greater access to what flows, over time. This natural tendency is summarized as the constructal law[14,15]. Here, we ask two questions:

First, what flow is spreading during solidification? It is not the solid, because the solid and its subcooled surroundings are motionless. The spreading flow is the flow of heat, which emanates from the solid surface and flows in all directions into the surroundings.

Second, what is the configuration of the heat flow system? We do not postulate the configuration (e.g. spheres in the JMA model). Instead, we rely on the physics principle[14,15] that the flow system generates and evolves its flow architecture in order for the solidification process to be the more "rapid" at every stage in its history. We show that although the solidification is triggered as small spheres around nucleation sites, at longer times the greater solidification rate is associated with needles and dendrites, in accord with common observations (e.g. Fig. 2[16]).

Results

Solidification begins at point-size nucleation sites around which the solid grows as tiny spheres. As shown later in the Discussion section, the spherical growth slows down and is replaced by needle-shaped growth, which is faster.

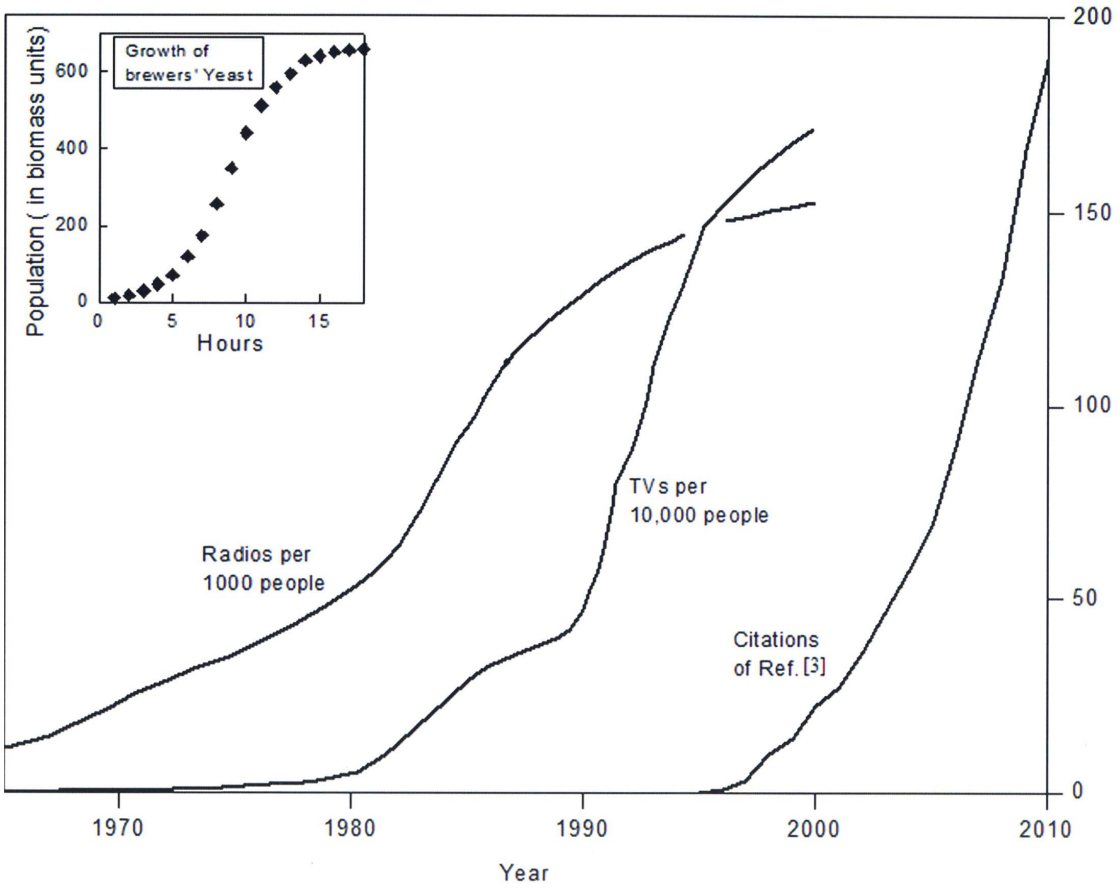

Figure 1 | Examples of S-curve phenomena: the growth of brewer's yeast[1], the spreading of radios and TVs[2], and the growth of the readership of scientific publications[3].

The transition from spherical to needle-shaped growth is in accord with the constructal law, and defines the early part of the S. Because most of the S-shape of the solidification curve is due to needle solidification, we start by examining the needle configuration.

Needle invasion. Consider the solidification of a volume of pure substance that is initially in a subcooled liquid state of temperature T_f, which is lower than the solidification temperature T_s. Along the axis of this volume grows a solid needle with a speed (V) that increases monotonically with the degree of subcooling ($T_s - T_f$), and which has been documented extensively (e.g. Refs. 17–21). The instantaneous length of the needle is x, and the length of the volume is L (Fig. 3).

Because of solidification, the needle grows in length and its older portions become thicker. In every stationary cross-section, the volume of solid is isothermal at T_s, and is proportional to the volume of liquid heated by the latent heat of solidification released on the solidification front,

$$B_s(t) \sim B_f(t) \tag{1}$$

In other words, the latent heat of solidification (h_{sf}) that was released on the periphery of the disc of solid is now the sensible heat of the annulus of heated liquid,

$$\rho_s h_{sf} D_s^2 \sim \rho_f c_f (T_s - T_f) D_f^2 \tag{2}$$

The scaling relation (2) is based on the assumption that $D_f \gg D_s$, and it yields the constant factor in the proportionality of Eq. (1), namely

$$\frac{D_s}{D_f} \sim \left[\frac{\rho_f c_f (T_s - T_f)}{\rho_s h_{sf}}\right]^{1/2} \tag{3}$$

The objective of this analysis is to predict the evolution of the solidification process, which means to predict the history of the volume of solid ($B_s \sim D_s^2 x$). Because of Eq. (3), the solid volume is proportional to the liquid volume heated by the heat of solidification, ($B_f \sim D_f^2 x$). Consequently, the shape of the history function $B_s(t)$ is the same as the shape of $B_f(t)$, where in accord with Eq. (3),

$$\frac{B_s}{B_f} \sim \frac{\rho_f c_f (T_s - T_f)}{\rho_s h_{sf}} = b \tag{4}$$

where b is constant. The time during which the liquid and solid thicknesses grow to the length scales D_f (t) and D_s (t) is

$$t = \frac{x}{V} \tag{5}$$

During this time, the liquid thickness grows by thermal diffusion,

$$D_f \sim (\alpha_f t)^{1/2} \tag{6}$$

where α_f is the liquid thermal diffusivity. From Eqs. (5) and (6) follows the history of the volume of heated liquid,

$$B_f \sim D_f^2 x \sim \alpha_f V t^2 \tag{7}$$

The first conclusion is that B_f and B_s increase in proportion with t^2, along the needle "invasion" curve shown in Fig. 4. The volume increase is accelerated in time, but it is not exponential. This behavior lasts until the needle invades the entire liquid volume, $x \sim L$, which happens during the invasion time

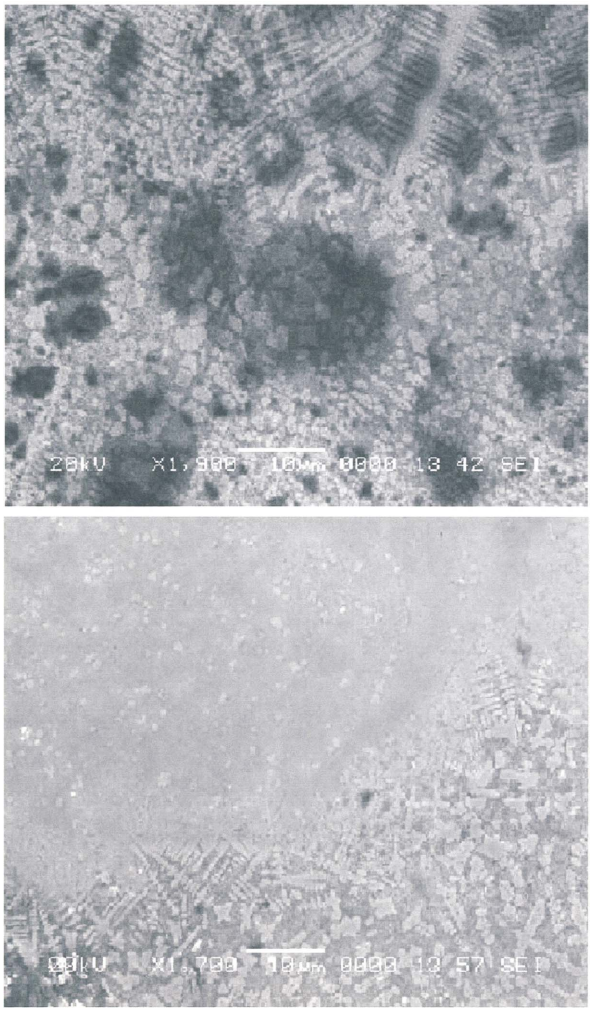

Figure 2 | **Dendritic solidification of Inconel 625 in the region close to the melt pool[16].**

$$t_i \sim \frac{L}{V} \tag{8}$$

when the liquid volume length scale is $B_{fi} \sim \alpha_f L^2/V$,with the corresponding solid volume B_{si} derived from Eq. (4).

Consolidation. Beyond the invasion time t_i, the solid and liquid volumes continue to grow in proportion with each other, but they grow *radially* laterally until D_f spreads over the entire subcooled liquid. This is the "consolidation" process. The growth of the liquid thickness is in accord with the solution to the problem of thermal diffusion around a line heat source of uniform and constant temperature (the needle, T_s) embedded in an infinite conducting medium (T_f)[22]:

$$\frac{T(r,t) - T_f}{T_s - T_f} = \frac{Ei(-r^2/4\alpha_f t)}{Ei(-\lambda^2)} \qquad (r \geq R) \tag{9}$$

$$R(t) = 2\lambda(\alpha_f t)^{1/2} \tag{10}$$

where R(t) is the radius of the solid cylinder, t = 0 is the start of the needle solidification process, and T(r, t) is the temperature in the liquid. The cylindrical geometry to which Eqs. (9) and (10) refer is visualized in the x = constant cut through the solid shown in Fig. 3. Ei is the exponential integral function

$$Ei(w) = \int_w^\infty \frac{e^{-y}}{y}\, dy \tag{11}$$

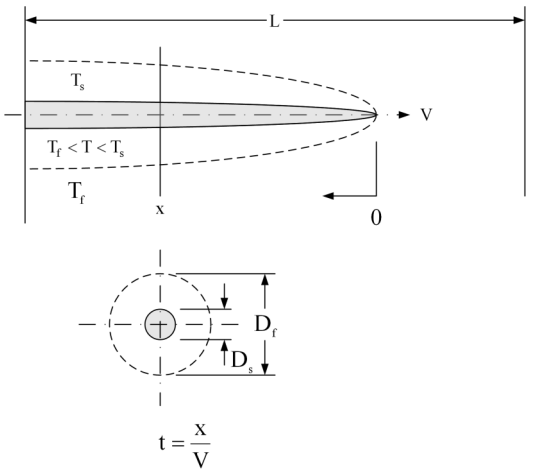

Figure 3 | **Needle generated by conduction from a solidifying body that grows to the left.**

while λ is a monotonic function of the liquid subcooling Stefan number [$Ste = c_f(T_s - T_f)/h_{sf}$], as shown in Fig. 5:

$$\lambda^2 \exp(\lambda^2) Ei(-\lambda^2) + Ste = 0 \tag{12}$$

The temperature distribution in the subcooled liquid is plotted in Fig. 5 for the case Ste = 1. The abscissa shows that the radial length scale (r) of the heated liquid increases as $2(\alpha_f t)^{1/2}$. The volume of liquid heated during the consolidation increases in proportion with the cross-sectional area of the annulus of heated liquid, namely $\pi(r^2 - R^2)$, which has the scale $\alpha_f t$.

The second conclusion is that the growth of B_f (or B_s) during consolidation process is proportional to t, which is slower than the t^2 growth during the invasion process. This accounts for the inflexion of the S curve, which is the beginning of the slowdown of solidification, Fig. 4.

Plateau. The liquid volume has two dimensions, the longitudinal length L aligned with the needle, and the lateral (radial) dimension Y, across the interstices. The time when the radial dimension of the heated liquid reaches Y is the consolidation time t_c,

$$t_c \sim \frac{Y^2}{\alpha_f} \tag{13}$$

which follows from writing $r \sim Y$, where $r \sim (\alpha_f t)^{1/2}$. After this event, the heated liquid (already Y thick) becomes warmer at a progressively smaller rate, as its average temperature rises to match the solidification temperature T_s. This final arc of the S-curve of solidification can be predicted as follows.

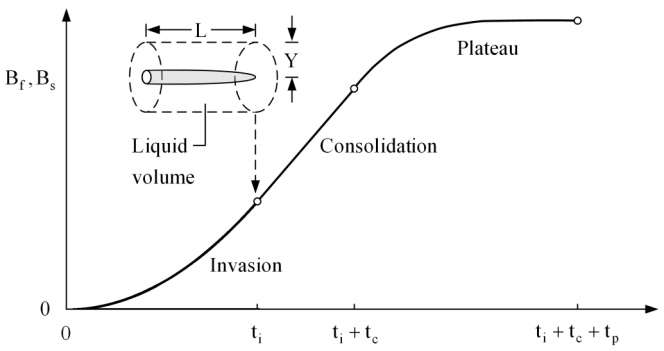

Figure 4 | **The history of the volume of heated fluid during the invasion and consolidation processes.**

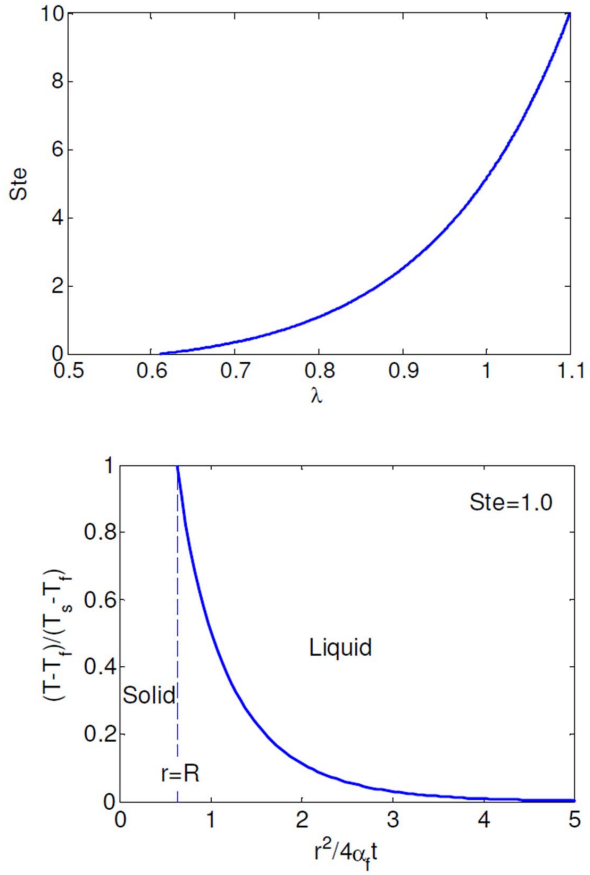

Figure 5 | The radial distribution of temperature in the subcooled liquid, and the λ (Ste) solution to Eq. (12).

The heat current flows from the solidification front across the Y-thick liquid of average temperature $T_l(t)$, and has the scale $k_f\pi D_s(T_s - T_l)/Y$, where it is assumed that $Y \gg D_s$. The heat current is equal to the rate at which the energy of the liquid layer increases, namely $\rho_f c_f \pi Y^2 dT_l/dt$. Integrating the resulting equation and invoking the initial condition $T_s - T_l \cong T_s - T_f$ at $t = t_i + t_c$, we obtain the decelerating rise of the liquid temperature,

$$\frac{T_s - T_l}{T_s - T_f} \cong e^{-(t - t_i - t_c)/t_p} \tag{14}$$

where t_p is the time scale of reaching the T_s plateau:

$$t_p = \frac{\rho_f c_f Y^3}{k_f D_s} \tag{15}$$

The heat current released at the solidification front is proportional to the temperature gradient across the Y-layer, therefore it has the same exponential decay as in Eq. (14). The same behavior belongs to the rate of solidification dB_s/dt, and consequently the history of the solid volume $B_s(t)$ has the flattening tendency sketched in Fig. 4.

Discussion

In summary of the preceding analysis, the history of needle solid volume is composed of three successive periods (invasion, consolidation, plateau), each with its own time scale: t_i, t_c and t_p. The analysis began with the needle invasion process, and it was based on the assumption that the solid is needle shaped, i.e. it is slender, not spherical. Why and under what conditions this assumption is correct is the foundation of the S-curve of solidification, and it is demanded by the constructal law.

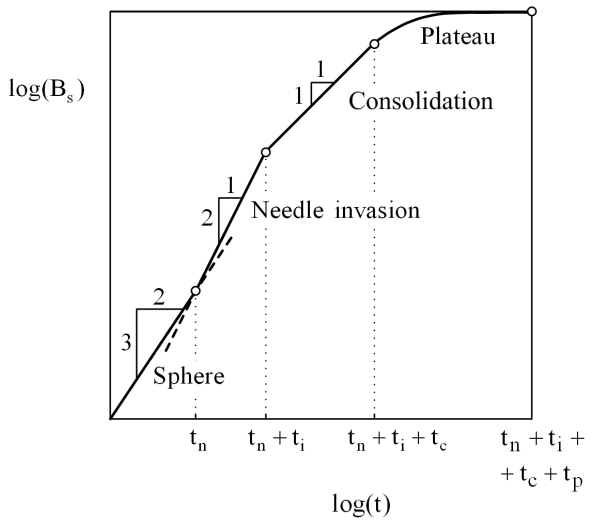

Figure 6 | The complete S curve of solidification. Note the early competition between the sphere and needle configurations in the pursuit of more rapid solidification. The last three regions (invasion, consolidation, plateau) are log-log representations of the S curve shown in Fig. 4.

Solidification begins at point-size nucleation sites, and for this reason the earliest shape of the solid is spherical, of diameter $D_s(t)$. The sphere is surrounded by an annulus of heated liquid of outer diameter $D_f(t)$, which increases in proportion with $(\alpha_f t)^{1/2}$. Equation (2) is replaced by

$$\rho_s h_{sf} D_s^3 \sim \rho_f c_f (T_s - T_f) D_f^3 \tag{16}$$

and leads to the conclusion that $D_s(t)$ and $D_f(t)$ increase proportionally, and

$$\left(\frac{D_s}{D_f}\right)^3_{\text{sphere}} \sim \left(\frac{B_s}{B_f}\right)_{\text{sphere}} \sim b \tag{17}$$

The solid volume $B_{s,\text{sphere}}$ (of order D_s^3) increases as

$$B_{s,\text{sphere}} \sim b(\alpha_f t)^{3/2} \tag{18}$$

The needle is the alternative configuration, which competes with the sphere. During the same time interval (0 – t), the needle would acquire the volume [cf. Eq. (7)]

$$B_{s,\text{needle}} \sim \alpha_f V t^2 b \tag{19}$$

The intersection of Eqs. (18) and (19) reveals the time scale of needle onset,

$$t_n \sim \frac{\alpha_f}{V^2} \tag{20}$$

where as shown in Fig. 6,

$$B_{s,\text{sphere}} > B_{s,\text{needle}}, \text{ if } t < t_n \tag{21}$$

$$B_{s,\text{needle}} > B_{s,\text{sphere}}, \text{ if } t > t_n \tag{22}$$

In conclusion, in the evolution of configuration the sphere is first and the needle next. Not the other way around. In accord with the constructal law, this sequence of heat flow designs facilitates more effectively the flow of heat toward equilibrium, i.e. this is the evolutionary design in which the solidification is more rapid.

The succession of four heat-flow configurations (Fig. 6) is why the history of the solidified volume is S shaped. The S curve is a power law $B_s \sim t^n$, where the exponent varies over time in this sequence:

n = 3/2, 2, 1 and finally n < 1. The early part of the S-curve is not an exponential.

1. Pearl, R. The growth of populations. *Quarterly Review of Biology* **51** (50th Anniversary Special Issue, 1926–1976), 6–24 (1976).
2. Easterly, W. *The White Man's Burden* (London, Penguin Books, 2006).
3. Bejan, A. & Lorente, S. The physics of spreading ideas. *International Journal of Heat and Mass Transfer* **55**, 802–807 (2012).
4. Hubbert, M. K. Energy from fossil fuels. *Science* **109**, 103–109 (1949).
5. Avrami, M. Kinetics of phase change II: transformation-time relations for random distribution of nuclei. *Journal of Chemical Physics*, **8**, 212 (1940).
6. Christian, J. W. *Theory of transformation in Metals and Alloys*, 2nd Ed. (Oxford, UK, Pergamon Press, ch. 10, p. 473, 1969).
7. Chen, H. S. Glassy metals. *Reports on Progress in Physics* **43**, 354–432 (1980).
8. Málek, J. The applicability of Johnson-Mehl-Avrami model in the thermal analysis of crystallization kinetics of glasses. *Thermochmica Acta* **267**, 61–73 (1995).
9. Zener, C. Theory of growth of spherical precipitates from solid solutions. *Journal of Applied Physics* **20**, 950–953 (1949).
10. Wert, C. A. Precipitation from solid solutions of C and N in α – iron. *Journal of Applied Physics* **20**, 943–949 (1949).
11. Turnbull, D. & Treaftis, H. N. Kinetics of precipitation of tin from lead - tin solid solutions. *Acta Metallurgica* **3**, 43–54 (1955).
12. Cahn, J. W. The kinetics of grain boundary nucleated reactions. *Acta Metallurgica* **4**, 449–459 (1956).
13. Aaron, H. B., Fainstein, D. & Kotler, G. R. Diffusion-limited phase transformations: a comparison and critical evaluation of the mathematical approximations. *Journal of Applied Physics* **41**, 4404–4410 (1970).
14. Bejan, A. *Advanced Engineering Thermodynamics*, 2nd ed. (New York, Wiley, 1997), ch. 13.
15. Bejan, A & Lorente, S. The constructal law and the evolution of design in nature. *Physics of Life Reviews* **8**, 209–240 (2011).
16. Taha-al, Z. Y., Hashmi, M. S. J. & Yilbas, B. S. Effect of WC on the residual stress in the laser treated HVOF coating. *Journal of Materials Processing Technology* **209**, 3172–3181 (2009).
17. Powell, G. L. F., Colligan, G. A., Surprenant, V. A. & Urquhart, A. The growth rate of dendrites in undercooled tin. *Metallurgical Transactions A* **8**, 971–973 (1977).
18. Huang, S.-C. & Glicksman, M. E. Fundamentals of dendritic solidification—II Development of sidebranch structure. *Acta Metallurgica* **29**, 717–734 (1981).
19. Liu, F. & Goldenfeld, N. Linear stability of needle crystals in the boundary-layer model of dendritic solidification. *Physical Review A* **38**, 407–417 (1988).
20. Ben Amar, M. Dendritic growth rate at arbitrary undercooling. *Physical Review A* **41**, 2080–2092 (1990).
21. Liu, Z.-K. & Chang, Y. A. On the applicability of the Ivantsov growth equation. *Journal of Applied Physics* **82**, 4838–4841 (1997).
22. Carslaw, H. S. & Jaeger, J. C. *Conduction of Heat in Solids* (Oxford UK, Oxford University Press, 1959).

Acknowledgments

The authors acknowledge the Deanship of Scientific Research, King Fahd University of Petroleum and Minerals, Dhahran, Saudi Arabia, for funding the project IN111042 during the course of this work.

Author contributions

A.B. did the research work in collaboration with the other three co-authors, wrote the manuscript and made Figures 1, 3, 4 and 6. S.L. did the research work in collaboration with the other three co-authors, wrote the manuscript and made Figures 1, 3, 4 and 6. B.S.Y. did the research work in collaboration with the other three co-authors, wrote the manuscript and made Figure 2. A.Z.S. did the research work in collaboration with the other three co-authors, wrote the manuscript and made Figure 5.

Additional information

Competing financial interests: The authors declare no competing financial interests.

How to cite this article: Bejan, A., Lorente, S., Yilbas, B.S. & Sahin, A.Z. Why solidification has an S-shaped history. *Sci. Rep.* **3**, 1711; DOI:10.1038/srep01711 (2013).